

Analysis of four point bending characteristic of composite assembled hollow slab using profiled steel wire mesh

Tran Duy Trinh¹, Dao Duy Kien^{1*}

¹Department of Civil Engineering, University of Technology and Education Ho Chi Minh City, No 1 Vo Van Ngan Street, Linh Chieu Ward, Thu Duc City, Ho Chi Minh City, Vietnam

KEYWORDS

Assembled hollow slab
Profiled steel wire mesh
Bending test
Ductility
Composite

ABSTRACT

Optimizing the performance of reinforced concrete structures by reducing mass, reducing component height, increasing ductility and flexibility, durability, fast construction, and environmental protection has always been the goal of countless studies related to reinforced concrete structures. In this study, 03 hollow slab plates, each slab has one different assembly combination, without beams, using profiled fiber wire mesh, assembled by assembling 12 small slab panels with dimensions of 2800x2000x300, 3000x1950x300 (mm), 2800x1950x300 (mm), respectively were put into 4-point bending for sagging behavior analysis, deformation, crack formation, analysis of slab plasticity. Using profiled steel wire mesh with a grid cell size of 12x12x1 (mm) and steel fiber diameter of 1mm can not only completely replace the reinforcement but also improve the slab's flexibility, flexibility, and toughness. In addition, the way the complex assembles small panels according to the working method also contributes to improving the behavior efficiency of the slab. The plasticity of slab specimens shows that arranging multiple layers of mesh involved in tensile resistance will increase the structure's load-bearing capacity, but the ductility of the structure decreases. The main reason is the use of cold-drawn steel fiber mesh to make reinforcement to bear the load because cold-drawn steel has high brittleness, so at a large load, pulling off steel layers occurs in a fast branch chain effect, thereby reducing the ductility of the structure. The results can be applied to the design of prefabricated concrete slabs and structures.

1. Introduction

Traditional reinforced concrete slabbing is the earliest option widely used in construction works today. It has the characteristics of being easy to manufacture and manufacture, taking advantage of available local raw materials, enhancing the rigidity of the load-bearing frame of the building, withstanding large loads, having high durability and resistance to aggressive factors from the environment, and less maintenance. However, one of the disadvantages of reinforced concrete slabs is that they have large, self-weight, small slab beam spans that thicken the column grid, limiting space expansion in the design. If it is necessary to increase the span of the slab beam, the size of the reinforcing structure must increase, thereby increasing the load transmitted to the column and foundation system of the building.

Due to the above disadvantages, many different slab options are being developed today to overcome the disadvantages of the whole block reinforced concrete slab plan. One of those options is a hollow slab structure. The hollow slab is a type of slab structure in which areas of material that are not or less involved in the working and bearing process of the structure are removed or replaced with hollow parts, thereby reducing the weight of the slab structure while still meeting the requirements of durable conditions (bearing capacity) and stable

conditions when using (deflection). Many structural options for hollow slabs have been proposed and put into use, such as bubble slab, flag slab, foam slab (3D slab, VRO slab), NEVO beamless hollow slab,...

Hollow slab structures bring many benefits because they have many preeminent features, such as flexibility in design and construction, efficient use, and economic efficiency. One of those solutions is to use small profiled steel fiber mesh to reinforce concrete materials (Ferrocement). This solution was proposed and put into use very early. Thanks to its relatively good strength and high impact resistance, steel fiber mesh concrete solutions were widely used in structural forms such as hulls, water tanks, and flower beds in the early period. The study combined experimentation and simulation with finite elements to assess the shear resistance of the added concrete layer on an existing hollow slab. It evaluated the simulation solution suitable for reality [1-6]. Chang-Hwan Lee *et al.* (2019) [7] conducted a study evaluating the bearing capacity of composite reinforced concrete hollow slabs (with additional reinforcement of shaped steel and corrugated iron). They investigated crack formation as well as sabotage when working at load levels. Carvalho *et al.* (2019) [8] carried out a study on the shear and penetration resistance of hollow slabs with different types of hollow building blocks and hollow section densities to assess

*Corresponding author: kiendd@hcmute.edu.vn

Received 29/10/2024, Revised 12/11/2024, Accepted 12/11/2024

Link DOI: <https://doi.org/10.54772/jomc.v14i02.795>

the suitability of design standards such as ACI 318-14, EN 1992-1-1 2004 and IS 456 2000 [9].

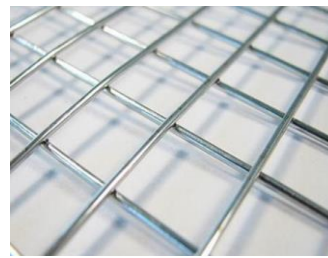
In addition to the application of distributed fiber reinforcement forms (mixed with foundation concrete materials in the process of concrete mortar kneading), around the 1970s, people proposed and conducted many studies on solutions to use shaped fiber mesh of all kinds to arrange into sheet structures, plates, and beams to enhance the bearing capacity of the structure and help limit the formation of cracks due to the relatively thick distribution of fiber reinforcement in the wire mesh. In those first years, steel fiber mesh was applied and used the most, and then new fibers were born, such as glass fiber, carbon fiber, polypropylene fiber, and basalt fiber. It has been considered and studied to replace steel fiber mesh in Ferrocement structures. When using profiled fiber mesh to enhance the bearing capacity of a structure that can withstand the impact forces when put into use, steel fiber mesh can be used to form a small steel column, from which it is possible to reduce or skip the use of large-diameter bar reinforcement to reinforce the bond claw. Steel fiber mesh concrete structures have been studied worldwide since the 1970s. In 1976, the International Ferrocement Information Center (IFIC) was established in Bangkok, Thailand, with the role of cooperating, providing information, and distributing studies on steel fiber concrete to all countries, as well as research units and technical consulting companies on steel fiber concrete (Ferrocement) [10-17].

Current hollow slabs use concrete, steel construction bars, and mold materials to create voids. For hollow slabs made of steel fiber concrete structures, the design only stops at using steel fiber mesh panels in flat form, so when the slab is under complex loads or at the time of manufacture, there will be some difficulties because the wire mesh is not shaped to help the hollow parts stabilize during construction. From the above issues and an additional option for the design and construction of a hollow slab structure, another form of hollow slab structure is proposed: a hollow slab combined from sand cement mortar using shaped steel fiber mesh. The steel fiber mesh used for sand cement mortar is a welded or knitted steel fiber mesh with a small size: mesh cell size from 10-40mm, steel fiber diameter from 0.3-2.0mm. This mesh type is lightweight, so the construction and installation will help reduce time and effort. On the other hand, the arrangement of the grid in the sheets is predetermined by mechanical machinery at the processing workshop, which helps to contribute to the industrialization of the wire mesh processing process, as shown in (Figure 1).

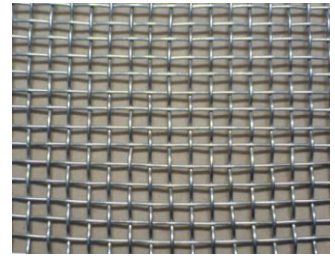
In order to properly evaluate the bearing capacity and analyze the behavior of the composite slab structure from sand-cement mortar panels reinforced with profiled steel fiber mesh, the experimental program was conducted on three hollow slab specimens; each specimen is a different combination from preformed steel fiber mesh units. The specimens will have different arrangements and combinations of basic plates to evaluate the most optimal combination plan. The results obtained from the experiment are compared with previous studies to

assess the structure being investigated and accomplish the following objectives: Analyze the behavior of essential sand-cement mortar when working in the overall structure—evaluation of the bearing capacity of composite hollow slab structures from sand-cement mortar reinforced with profiled fiber mesh. The results are expected to be achieved, thereby proposing the applicability of this type of structure in the design and construction of works in the near future.

Compared to traditional hollow slab structures, the composite hollow slab structure will have more advantages: (i) in terms of construction methods: more accessible in construction due to the use of preformed mesh assemblies, (ii) in economy: due to the use of prefabricated components for assembly, it will reduce the formwork area, shorten the construction time, the primary sheet is reinforced with a small-sized steel fiber mesh, so the volume of steel materials used will be significantly reduced, and the small-sized fiber mesh has high flexibility, low self-weight, so it is easy to process, shape and erect without spending too much effort like traditional reinforcement, thereby contributing to increasing the economy of this type of structure, (iii) increasing industrialization in the production and erection process: Due to the use of basic sheets of the same size to assemble the combination, the steel fiber mesh for these plates can be processed industrially and the plate casting process is carried out according to the industrial production help increase productivity, contribute to reducing the cost of products.



a) Welded wire mesh



b) Lưới inox



c) Hexagonal wire mesh



d) Diamond trellis

2. Experimental program

2.1 Hollow slab structures working mechanism

Hollow slab structures can be analyzed into I- or T-beam structures in the form of 1 direction (for 1-way working slab version) or two directions (2-way working slab version). For rectangular (or square)

mesh wire fiber mesh, when the mesh fiber method is arranged to coincide with the bearing direction of the structure, then the mesh fibers can be considered as reinforcement (microfiber reinforcement) in concrete. These reinforcements will participate in tensile or compressed concrete during the process of the component participating in loading. Because mesh fibers are considered reinforcement, according to concrete structure design standards can be used to calculate, design, and test components like conventional reinforced concrete structures. With the structure of a shaped steel mesh system with tensile resistance combined with compressible cement mortar materials and lighter than conventional concrete materials, the bearing capacity and stability of the whole structural system are completely guaranteed through these two materials. Therefore, when the structure works, the behavior of the whole structure depends a lot on the component materials and other related conditions such as size, content, and the arrangement of mesh fiber reinforcement to participate in bearing along with the tone of the slab. Therefore, the change in mortar strength, wire mesh content, combinations of single mesh elements, and the interaction between constituent elements directly affect the bearing capacity and the behavior of the whole structural system. The objectives set at the beginning of the project are based on the results of experiments and the results of simulating the topic of conducting surveys in aspects such as: Determine the bearing capacity, displacement and deformation of the combinatorial slab structure.

- Surveying of the working between the wire mesh system used and mortar materials.
- Whether the durability of the structure is guaranteed.
- Analyze the general working of the steel fiber mesh system and sand cement mortar, check the bearing capacity of the combined slab structure.
- It is expected that the results will be achieved, suggesting the applicability of this type of link in the near future.

2.2. Experimental specimen

The experiment will be conducted on three primary specimens, which are three cases of different combinations of single panels; each slab will be combined from 24 single mesh clusters and together in different combinations; the hollow part in the middle will use foam to create hollows for the slab structure when pouring concrete.

Since there are no specific standards to guide the implementation of design for laboratory specimens, it is essential to establish experimental specimens based on practical applications, combined with an initial assessment of structural types and conditions at the laboratory. The general shape of the experimental specimen is (Table 1).

The specimen used for the experiment is designed based on the actual situation. The parameters of materials and structure of each specimen plate are shown in detail in the (Figure 2), (Figure 3), (Figure 4) below.

Table 1. Description of the experimental specimen.

Specimen	Type 1	Type 2	Type 3
Section (mm)	2800x2000x300	3000x1950x300	2800x1950x300
Mortar strength f_{ck} (MPa)	30	30	30
Steel fiber mesh size (mm)	12x12xØ1	12x12xØ1	12x12xØ1
Number of specimens unit	12	12	12

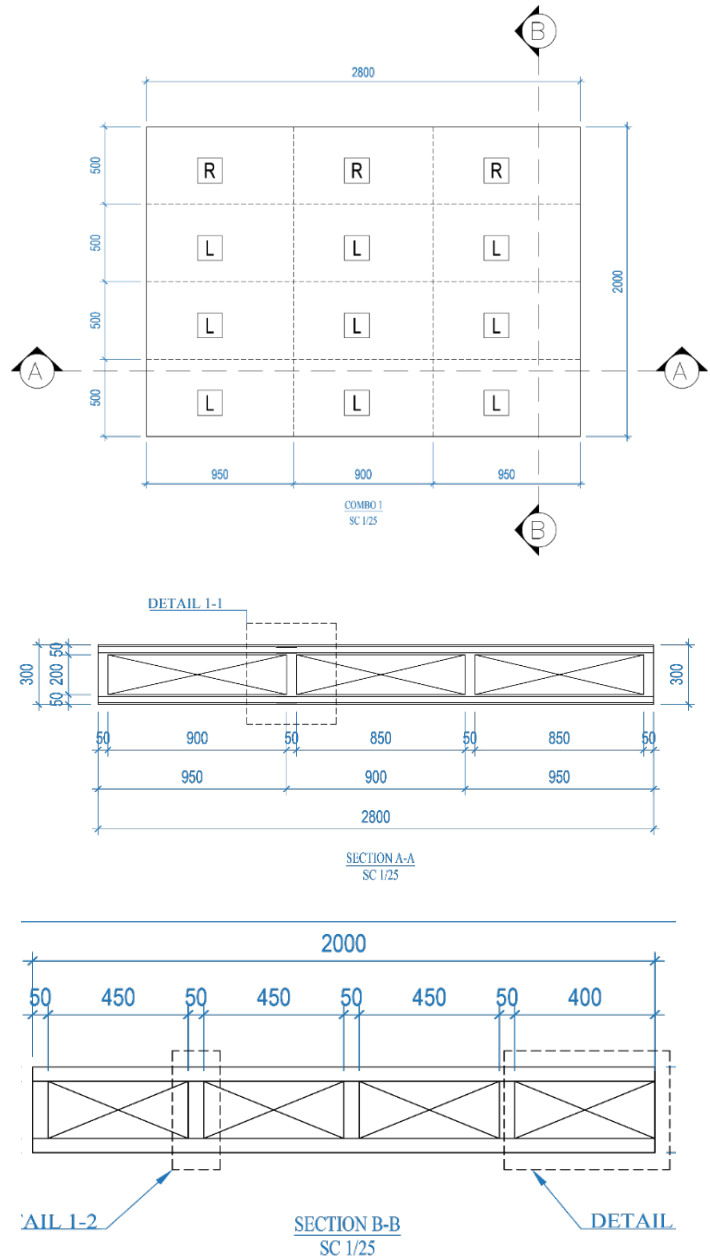


Figure 2. Layout and details of the slab Type 1.

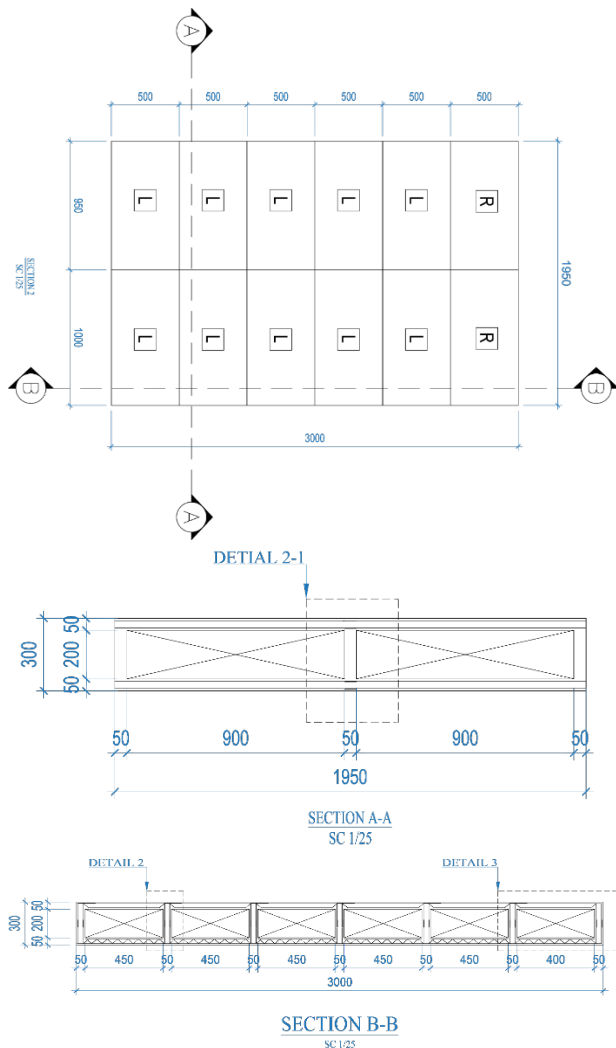


Figure 3. Layout and details of the slab Type 2.

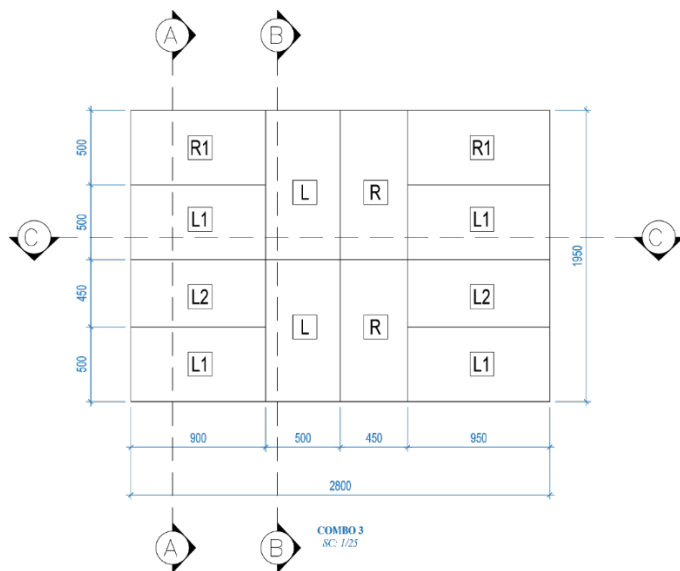


Figure 4. Layout and details of the slab Type 3.

2.3. Material properties

Due to limited conditions, the project is only surveyed based on three slab specimens, so all three specimens will share the same grade of mortar mixing. The strength of the mortar selected for the test specimen is M300 mortar grade, equivalent to a cubic strength test specimen with an edge size reaching the destructive load with a stress of 30 MPa. In addition to the test of the compressive strength of the mortar specimen for the evaluation of the correct behavior, the specimen was also tested to determine many other parameters to serve the simulation of finite elements in the future, such as an experiment to determine the elastic modulus, Poisson coefficient, etc. deformation stress relationship line, tensile strength when bending, tensile stress behavior line – crack expansion. In order to determine the tensile strength of fct bending (MPa), the Rilem beam bending experiment is used. The specimen used in the experiment was a mortar specimen with a length of 600mm and a square cross-section of 150mm. Since the tensile capacity of the mortar is not high, in order to be able to accurately measure the results and observe the formation and development of the crack, the loading must take place very slowly, and the load increase is minimal, as shown in (Figure 5).

The results of the experiment, after being collected and processed, are recorded according to (Table 2).

2.4. Fabrication process

Many factors affect the behavior of the structure; however, within the limits of the topic, the topic only surveys some of the main parameters as follows: In this project, the survey will be conducted on three types of hollow slab combinations marked TH1, TH2, TH3, the parameters of the test specimen are presented in (Table 1).

After installing the mesh further under the slab, as shown in (Figure 6), proceed to install the shaped foam blocks and then install the mesh on the foam blocks and finish.

After the formwork is ready, the mixing and mortuating of the specimen is started. According to the specimen slab size, there will be a volume of 0.9 m³ for each slab combination. The mortar used is a self-flowing mortar with high flexibility to fill and blanks between the welded wire mesh strands. When pouring the mortar, it is necessary to combine it with a vibrating compactor so that the mortar can be easily moved and fill the empty areas for the slab. At the end of this work, the mortar is leveled with a flying plane and a scrubbing table to create flatness for the specimen surface, and maintenance is carried out 2 times a day for seven consecutive days before removing all plastic bags, clothes and formwork, as shown in (Figure 7).



Figure 5. Experiment to determine material properties.

Table 2. Results of compression experiments.

Material Concrete	Force P(kN)	Compressive Strength f_c (MPa)	Tensile strength when bending f_{ct} (MPa)	Elastic modulus E_c (MPa)	Elastic Strain Limit ϵ_{elas} (‰)	Maximum compression limit ϵ_{limit} (‰)
	600	33	2.86	22×10^3	1	2554
Fiber diameter 1,2 mm (10x10)	Flow Limit f_y (MPa)		Endurance Limits f_u (MPa)		Plastic deformation ϵ_y (‰)	Elastic Module E (MPa)
	450		680		2.3	20×10^4



Figure 6. Steel grating after bending forming.



Figure 7. Completed specimens.

3. Testing program

Twenty-eight days after casting, the specimen was put into the experiment. The 3-point bending point is applied in this experiment; based on the conditions in the laboratory and referring to previous documents, the experimental is detailed in (Figure 8).

All measuring instruments are installed, checked, and calibrated carefully before experimenting. The computer system records the test data automatically with a frequency of 1 (times/s).

An automatic hydraulic pump will load the hydraulic jack; the loading speed will be calculated and selected to suit the load capacity of the slab specimens. Choosing the appropriate loading rate not only helps to control the experiment better and avoid sudden specimen damage but also helps the process of recording data more fully to serve the process of testing and evaluating experimental specimens.

The loading rate for each test slab specimen is presented in (Table 3).



a. Data Logger



b. Installation of LVDT1, LVDT2, LVDT3

Figure 8. Placement of displacement measuring devices on slabs.



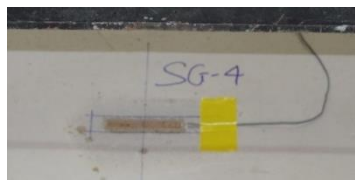
a) Strain Gauge SG1



b) Strain Gauge SG2



c) Strain Gauge SG3



d) Strain Gauge SG4

Figure 9. Installing Strain Gauges on Slabs.

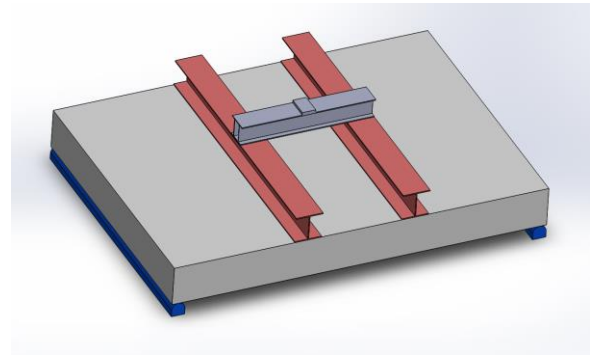


Figure 10. Arrangement of the test slab specimens.

Table 3. Load capacity and loading speed of slab.

Specimen	Flexible Design Moment M_n	Moment allows according to the bearing capacity [M]	Allowable load by design [P]	Loading speed
	kNm	kNm	kN	kN/s
Slab-Type 1	15.49	10.07	67.64	1
Slab-Type 2	7.89	7.1	13.2	0.2
Slab-Type 3	7.89	7.1	13.2	0.2

4. Results and discussion

4.1. General results

By the Data Acquisition data collection system, the data to be measured is summarized according to (Table 4).

Table 4 shows that the arrangement of additional layers of load-bearing mesh in the tensile zone (Type1 slab has three layers of load-bearing mesh in the tensile zone, of which Type2 slab and Type3 slab only have one layer) will increase the bearing capacity of the slab to the specific that the Type1 slab has more bearing capacity than the Type2 slab. The Type3 slab is 197.82 kN, about 74.2%, and 186.56, about 69.78%. Slabs No. 2 and No. 3 have the same cross-section at the middle span position, but the bearing capacity of No. 3 is about 14% higher

than No. 2 is 11.26 kN. In comparison, the deflection of Type 3 slab tubers is 0.7mm less than that of Type 2 slab by about 11.38%, which shows that the arrangement of different single mesh combinations will give the bearing capacity different forces. The effect of the combination of the dimensions of the grid units constitutes the slab combination. It

is essential to establish experimental specimens based on practical applications, combined with an initial assessment of structural types and conditions at the laboratory.

Table 4. Experiment Results.

Specimen	Pmax (kN)	Deflection (mm)	Proportional deflection	Elastic moment according to experiments (kNm)	Elastic moment by design (kNm)	Destructive form
Slab-Type 1	266.60	14.72	$\frac{5.5}{1000}L_0$	39.43	15.49	Plastic Destruction
Slab-Type 2	68.78	6.15	$\frac{2.3}{1000}L_0$	8.74	7.89	Plastic Destruction
Slab-Type 3	80.04	5.45	$\frac{2.0}{1000}L_0$	11.47	7.89	Plastic Destruction

4.2. Evaluate the deflection of the specimen plate.

The deflection of the specimen plate is recorded by 3 LVDTs, namely LVTD1, LVTD2, and LVTD3, installed at positions of 1.35m, 0.9m, and 0.45m from the pillow and in the middle of the slab span. Therefore, the analysis and comments for the specimen's behavior according to the deflection are drawn using a graph showing the relationship between force deflection and deflection at each load level.

The force-deflection relationship diagram shown in (Figure 11) shows the rationality in the working of the hollow slab; that is, the displacement of the beam at the cross-section far from the backrest is greater than the cross-section near the backrest. Figure 12 shows that the displacement of the slab varies with each load level; the displacement

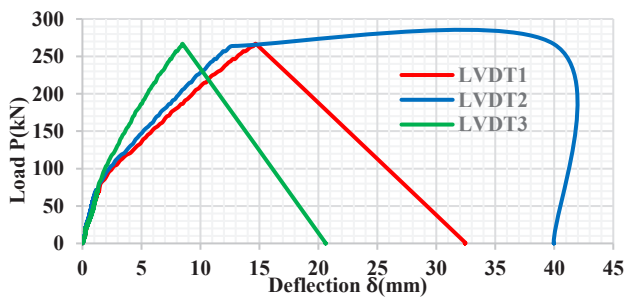
increases significantly from the load level $P = 60\%P_{max}$, especially when this load level is significantly displaced. This can be explained by the slab moving from the elastic to the flexible working stage.

4.3. Comparison of deflection between specimens

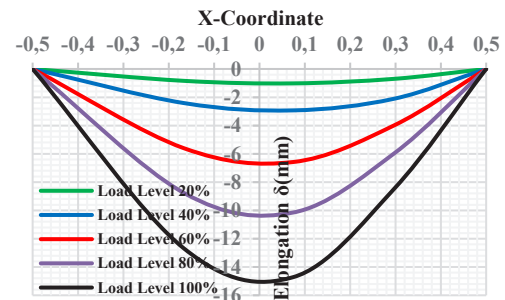
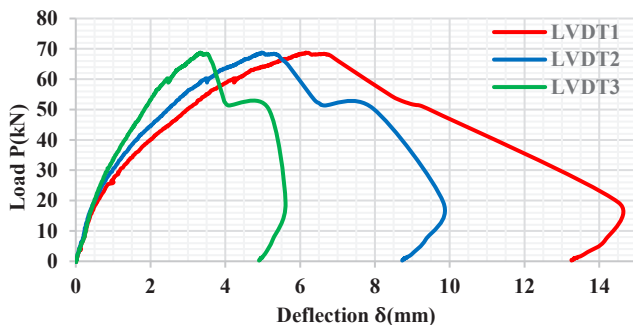
Like ordinary reinforced concrete components, the deflection of the specimen plate is influenced by many factors according to the formula:

$$f = \frac{5}{384} \times \frac{qL^4}{EI}$$

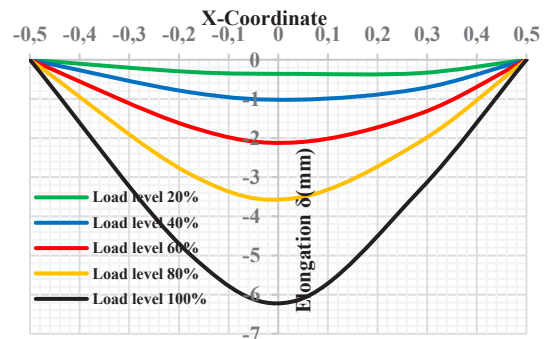
According to this survey, the bearing capacity and deflection of the specimen plate are described.

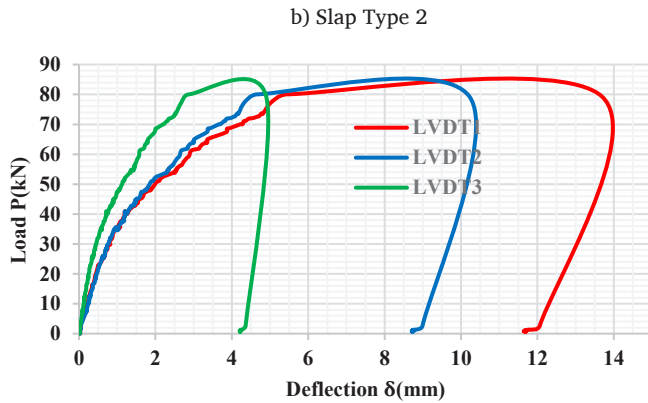


a) Slab Type1



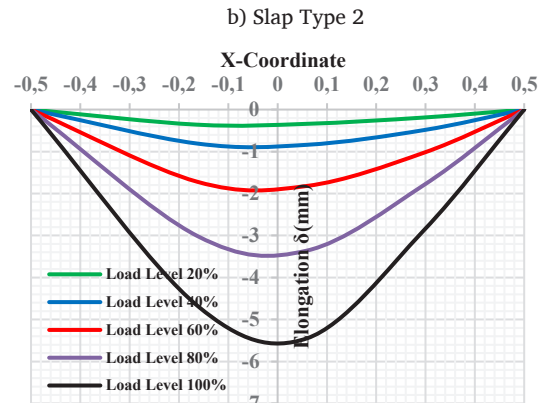
a) Slab Type1





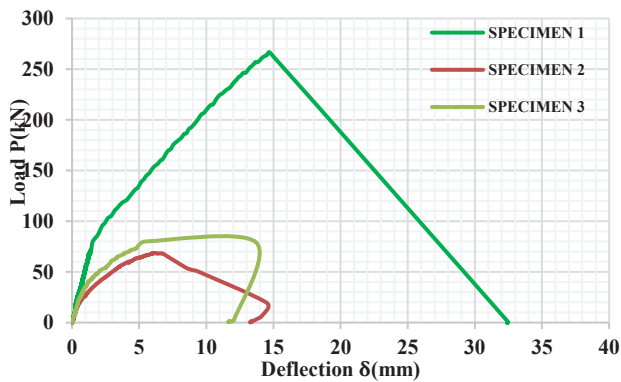
c) Slab Type 3

Figure 11. Force-deflection relationship.

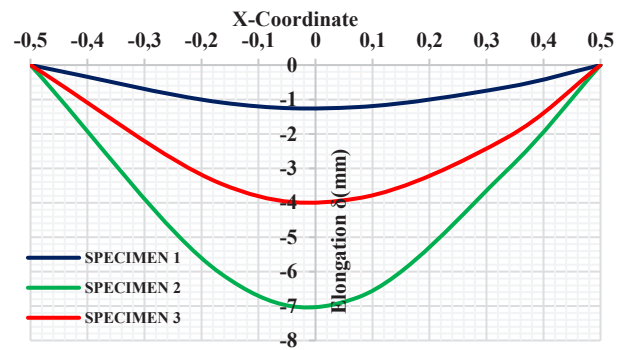


c) Slab Type 3

Figure 12. Deflection at load level.



a) Force-deflection relationship



b) Beam length deflection

Figure 13. Comparison of the deflection of slabs.

4.4. Deformation and destructive form of the specimen plate.

4.4.1. Strain of concrete slab

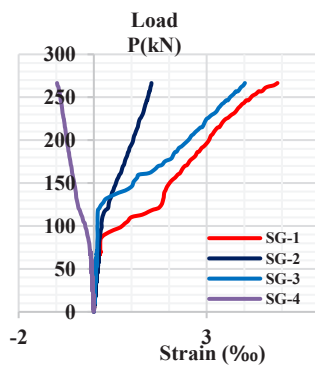
The deformation of the concrete slab is surveyed by strain gauges SG1, SG2, SG3, and SG4, which are pasted on the upper and lower sides of the slab; the evaluation is through the force-deformation relationship chart of the concrete slab figure.

The figure shows that the top of the compression-resistant slab and the bottom of the tensile slab show the true nature of the reinforced concrete structure when bent.

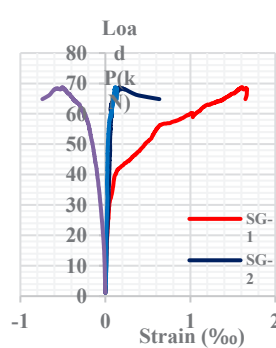
The stresses and deformations that arise when the specimen plate is under load can be calculated according to the following formula:

$$\delta = \frac{P}{A} \quad \varepsilon = \frac{\delta}{E} = \frac{P}{AE}$$

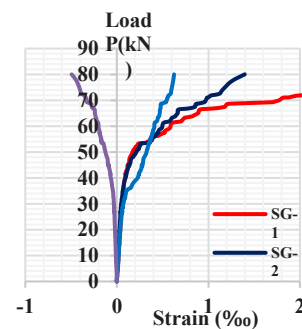
According to this survey, the bearing capacity and deformation resistance of the plate are described.



a) Slab Type 1



b) Slab Type 2



c) Slab Type 3

Figure 14. Strain of concrete slab.

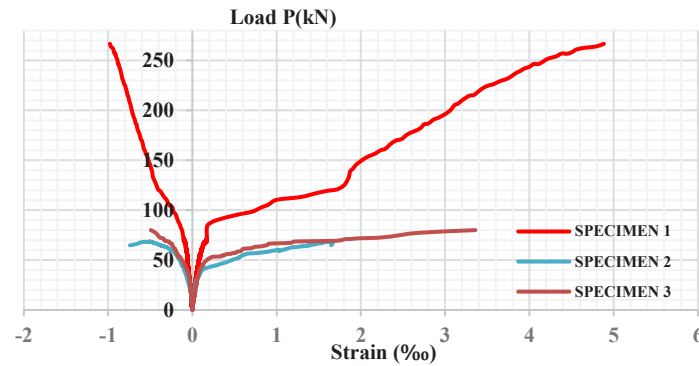


Figure 15. Comparison of concrete slab deformation.

4.4.2. The destructive form of hollow slab structures.

At the end of the destructive experiment of all three slab specimens, as observed, the vandalism occurred because the load-

bearing reinforcement in the tensile area was melted and broken, leading to the slab specimen breaking near the center of the two supporting pillows. This is in line with the design calculation so that the slab template can work and vandalize in the form of plastic vandalism.



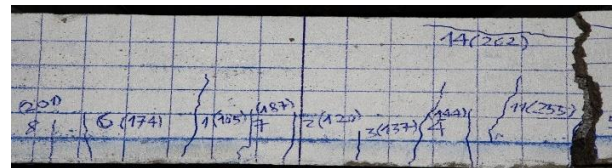
a) The left edge



d) The right edge



b) The cracks on the left edge



e) The cracks on the right edge



c) The left edge



f) the right edge

Figure 16. Slab Type1 specimen after performing the experiment.

5. Conclusion

Through an experimental survey on three specimens of hollow slabs made from cement mortar kettles cut using shaped steel fiber mesh, each slab specimen conducts a change of specific factors to analyze the influence of these factors on the behavior of hollow slabs using shaped steel fiber mesh. With the results obtained from the topic, I would like to propose some conclusions as follows:

- The content of steel fibers participating in the bearing (the steel fibers are stretched and ensure the anchor throughout) affects the bearing capacity of the slab specimen. Slabs with a high content of steel fibers participating in the bearing (Slab- Type1) will have a higher load capacity than those with less steel fibers participating.

- The content of steel fibers participating in the increased bearing also increases the hardness of the slab structure. The increase in the hardness of the slab structure will reduce the deflection at the

same level of scanning load as low-content slab specimens, increasing the load of cracks.

- Single tiles are not equal in size on two sides, from which the combination of arranging and arranging different tiles will produce slab specimens with different hardness, leading to the load capacity of the rigid slab specimens changing accordingly.

- The slab is arranged with many tiles with a long side and a single cell in the middle with the most bending direction, which will give a hefty load capacity and low deflection (because the long side, single cell has a larger rigid cell, and the short side with the exact width of the slab strip).

- The ribs along the long side of the single cell are also arranged with steel mesh, thereby increasing the cutting resistance for the slab; the long side of the single cell coincides with the bending direction.

- The cross-section on both sides of the single cell is different due to the modular structure of the 1-cell grid assembly. All the layout layers will be serialized when the overlapping position is located in the short edge position. In contrast, for the edge of the nest, only the outermost mesh layer can be connected (due to flank entanglement). Therefore, the bearing capacity depends on the slab cell cross-section compared to the maximum load-bearing cross-section.

- Concrete structures with reinforcement of steel fiber mesh have been researched and applied for a long time. The making barbells for thin-walled structures or non-standard artistic architectural works is easy.

- Behaves according to the working conditions according to the experiment; the slab structure can withstand large loads, has a low deflection, and is lightweight due to hollowing out the core near the neutral axis. Therefore, the hollow slab structure using this shaped steel fiber mesh can be applied entirely.

Acknowledgments This work belongs to the project grant No: T2024-02HVCH. funded by Ho Chi Minh City University of Technology and Education, Vietnam.

References

- [1] C. D. Tien, P. V. Khoan and L. Q. Hung, "Final report of Economic - Technical project for anti-corrosion and protection of reinforced concrete works in coastal areas," *Vietnam Institute for Building Science and Technology (IBST)*, vol. 11, pp. 78-88, 2003.
- [2] N. N. Thang, "Application study of calcium nitrite as an additive to inhibit reinforcement for reinforced concrete in Vietnam," *Vietnam Institute for Building Science and Technology (IBST)*, vol. 3, pp. 44-47, 2006.
- [3] J. P. Ollivier and A. Vichot, "La durabilité des bétons : bases scientifiques pour la formulation de bétons durables dans leur environnement/ sous la direction de Jean-Pierre Ollivier et Angélique Vichot," *École française du béton*, vol. 1, p. 868, 2008.
- [4] Training and retraining materials on corrosion test for concrete and reinforced concrete (Training program Project 1511), Vietnam Ministry of Construction, 2016.
- [5] Vietnam Standards, TCVN 9348:2012 - Reinforced concrete - Determining corrosion activity of reinforcing steel - Potential method, 2012.
- [6] A. Kivell, A. Palermo and A. Scott, "Effects of Bond Deterioration due to Corrosion in Reinforced Concrete," *Proceedings of the Ninth Pacific Conference on Earthquake Engineering*, Auckland, New Zealand, 14-16 April, 2011.
- [7] Z. H. Wang, L. Li, Y. X. Zhang and W. T. Wang, "Bond-slip considering freeze-thaw damage effect of concrete and its," *Engineering Structures*, vol. 201, p. 109831, 2019.
- [8] E. P. Carvalho, E. G. Ferreira, J. Cunha, C. Rodrigues and N. Maia, "Experimental Investigation of Steel-Concrete," *Latin American Journal of Solids and Structures*, vol. 14, pp. 1932-1951, 2017.
- [9] American Concrete Institute, ACI 318 (2019): Building Code Requirements for Structural Concrete and Commentary, 2019.
- [10] F. Li and Y. Yuan, "Effects of corrosion on bond behavior between steel strand and concrete," *Construction and Building Materials*, vol. 38, pp. 413-422, 2013.
- [11] A. Nanni, M. M. Al-Zaharani, S. Al-Dulaijan and C. Bakis, *Bond of reinforcement to concrete – experimental*, London: E and FN Spon, 1995.
- [12] L. Malvar, *Bond stress-slip characteristics of FRP rebars*. Technical Report TR 2013-SHR, California: Naval Facilities Engineering Service Center, Port Hueneme, February 1994.
- [13] V. Karbhari and M. Engineer, "Effect of Environmental Exposure on the External Strengthening of Concrete with Composites-Short Term Bond Durability," *Journal of Reinforced Plastics and Composites*, vol. 15, pp. 1194-1212, 1996.
- [14] J. G. Dai, W. Y. Gao and J. G. Teng, "Bond-Slip for FRP Laminates Externally Bonded to Concrete at Elevated Temperature," *Journal of Composites for Construction*, vol. 17, no. 2, pp. 217-228, 2013.
- [15] D. A. Moran and C. P. Pantelides, "Stress-strain for fiber-reinforced polymer-confined concrete," *Journal of Composites for Construction*, vol. 6, no. 4, pp. 233-240, 2002.
- [16] K. A. Soudki and F. G. Mark, "Freeze-thaw response of CFRP wrapped concrete," *Concrete International*, vol. 19, no. 8, pp. 64-67, 1997.
- [17] B. S. Pantazopoulou, "Repair of corrosion damaged columns with FRP Wraps," *Journal of Composites for Construction*, vol. 2, pp. 3-11, 2001.